BJP BRITISH JOURNAL OF PHARMACOLOGY

BPS BRITISH PHARMACOLOGICAL SOCIETY

British Journal of Pharmacology (2010), 159, 304–315

0007-1188/09
www.brjpharmacol.org

RESEARCH PAPER

Blebbistatin inhibits contraction and accelerates migration in mouse hepatic stellate cells

Zhenan Liu[1]*, Leo A. van Grunsven[1]*, Elke Van Rossen[1], Ben Schroyen[1], Jean-Pierre Timmermans[3], Albert Geerts[1,†] and Hendrik Reynaert[1,2]

[1]*Departments of Cell Biology and* [2]*Physiology, Vrije Universiteit Brussel, Brussels, Belgium;* [3]*Laboratory of Cell Biology and Histology, Department of Veterinary Sciences, University of Antwerp, Antwerp, Belgium.*

Background and purpose: Blebbistatin, an inhibitor of myosin-II-specific ATPase, has been used to inhibit contraction of invertebrate and mammalian muscle preparations containing non-muscle myosin. Activated hepatic stellate cells have contractile properties and play an important role in the pathophysiology of liver fibrosis and portal hypertension. Therefore, hepatic stellate cells are considered as therapeutic target cells. In the present study, we studied the effect of blebbistatin during the transition of mouse hepatic stellate cells into contractile myofibroblasts.
Experimental approach: Effects of blebbistatin on cell morphology were evaluated by phase contrast microscopy. Cell stress fibres and focal adhesions were investigated by dual immunofluorescence staining and visualized using fluorescence microscopy. Contractile force generation was examined by silicone wrinkle formation assays and collagen gel contraction assays. Intracellular Ca^{2+} release in response to endothelin-1 was measured by using Fluo-4. Cell migration was measured by wound healing experiments.
Key results: In culture-activated hepatic stellate cells, blebbistatin was found to change both cell morphology and function. In the presence of blebbistatin, stellate cells became smaller, acquired a dendritic morphology and had less myosin IIA-containing stress fibres and vinculin-containing focal adhesions. Moreover, blebbistatin impaired silicone wrinkle formation, reduced collagen gel contraction and blocked endothelin-1-induced intracellular Ca^{2+} release. Finally, it promoted wound-induced cell migration.
Conclusions and implications: By inhibiting myosin II ATPase, blebbistatin has profound effects on the morphology and function of activated hepatic stellate cells. Our data suggest that myosin II could be a therapeutic target in the treatment of liver fibrosis and portal hypertension.
British Journal of Pharmacology (2010) **159,** 304–315; doi:10.1111/j.1476-5381.2009.00477.x; published online 18 December 2009

Keywords: blebbistatin; myosin; hepatic stellate cells; contraction; migration; non-muscle myosin; α-SMA; stress fibres

Abbreviations: $[Ca^{2+}]_i$, intracellular Ca^{2+}; ECM, extracellular matrix; ET-1, endothelin-1; HSC, hepatic stellate cell; PBS, phosphate buffered saline; α-SMA, α-smooth muscle actin

Introduction

Hepatic stellate cells (HSCs) are located in the perisinusoidal space of Disse and represent 5–8% of cells in the normal liver. They play a pivotal role in vitamin A metabolism, in synthesis and degradation of extracellular matrix (ECM) and in regulation of sinusoidal blood flow (Geerts, 2001). Upon liver injury, they undergo transition into α-smooth muscle actin (α-SMA)-expressing myofibroblasts, which are characterized by loss of stored vitamin A, increased synthesis of collagen and α-SMA, reorganization of the actin cytoskeleton and increased deposition of ECM components. HSCs migrate to sites of inflammation and produce collagen and ECM constituents during the wound healing process, ultimately resulting in hepatic fibrosis and cirrhosis (Friedman, 2000; Geerts, 2001). They play an important role in the pathophysiology of fibrosis and portal hypertension and the paradigm of HSC activation provides an important framework for defining therapeutic targets (Gressner, 1991; Rockey and Weisiger, 1996; Geerts, 2001; Rockey, 2001; Reynaert *et al.*, 2002; Friedman, 2008). Myosins, which are actin-based motor

Correspondence: Hendrik Reynaert, Department of Cell Biology, Faculty of Medicine and Pharmacy, Vrije Universiteit Brussel (V.U.B.), Laarbeeklaan 103, 1090 Brussels, Belgium. Email: hendrik.reynaert@uzbrussel.be
*Contributed equally to the paper.
†Professor Geerts passed away during the completion of the study.
Received 29 April 2009; revised 6 July 2009; accepted 12 July 2009

proteins, play multiple vital roles in many different cell types, such as cardiomyocytes, kidney, neuronal and astrocytoma cells (Sellers, 2000; Guha *et al.*, 2005; Dou *et al.*, 2007; Haviv *et al.*, 2008; Salhia *et al.*, 2008). Specific inhibitors of myosin–actin interaction may provide insight into potential novel therapeutic approaches.

Blebbistatin was identified as a non-muscle myosin II-specific inhibitor (Straight *et al.*, 2003), although smooth muscle myosin and some non-conventional myosins (I, V and X) have been reported to be minimally influenced as well (Limouze *et al.*, 2004). Blebbistatin is cell-permeable and inhibits myosin function during cell division and motility in different cell types, such as neuronal cells, astrocytoma cells and vascular smooth muscle cells (Guha *et al.*, 2005; Shu *et al.*, 2005; Zhang and Rao, 2005; Calaminus *et al.*, 2007; Rosner *et al.*, 2007; Salhia *et al.*, 2008; Wang *et al.*, 2008). It further inhibits contraction of invertebrate and mammalian muscle preparations containing non-muscle myosin (Katayama *et al.*, 2006; Dou *et al.*, 2007; Fedorov *et al.*, 2007; Rosner *et al.*, 2007; Farman *et al.*, 2008; Salhia *et al.*, 2008). Little is known about the effects of blebbistatin on mouse HSCs, which are considered therapeutic target cells for liver fibrosis and portal hypertension (Reynaert *et al.*, 2002; Friedman, 2008). Migration and contraction are characteristic of activated HSCs, which are important for the formation of fibrous septa and the development and severity of portal hypertension (Friedman, 2003). Using blebbistatin we investigated whether non-muscle myosin II plays a role during the *in vitro* transdifferentiation of HSCs and in the contractility and migration of activated HSCs.

Methods

Isolation and culture of mouse HSCs

All animal care and experimental procedures were according to the institution's guidelines for the care and use of laboratory animals in research and this study was approved by the local ethical committee. All procedures were performed with animals under nembutal anaesthesia. HSCs used in this study were isolated by a modified collagenase-pronase digestion method as previously described (Reynaert *et al.*, 2001; Uyama *et al.*, 2006). About 1.5×10^6 freshly isolated HSCs were plated on 10 cm petri-dishes. To analyse activated HSCs, cells were trypsinized and replated when they had reached confluency after 5–6 days.

Western blot analysis

Cells were homogenized in sample buffer (62.5 mM Tris-HCl, pH 6.8, 2% SDS, 10% glycerol and proteinase inhibitor added before use), boiled for 10 min, sonicated and boiled for 15 s. Protein concentration was determined using the BCA protein assay kit (Pierce, Rockford, Illinois, USA). 10 μg samples in loading buffer with β-mercaptoethanol were loaded and separated by SDS-PAGE, then electroblotted onto polyvinylidene difluoride membrane (Millpore, Bedford, MA, USA). After blocking with 5% skim milk, 0.05% Tween 20 in PBS at room temperature for 1.5 h, the upper part of the blot was probed with primary antibodies to NMMHC-II isoforms, the lower part of the blot was incubated with primary antibodies to actin isoforms for 2 h at room temperature. The blots were washed and incubated with secondary antibodies for 1 h at room temperature. Proteins were detected by enhanced chemiluminescence using ECL substrate (Amersham, Rosendaal, the Netherlands).

Phase contrast and fluorescence microscopy

Cells were cultured in absence or presence of blebbistatin (50 μM) for 2 h at the indicated days and then photographed. For immunodetection, cells were plated on non-coated coverslips in 24-well plates and fixed for 10 min in acetone/ethanol (3:1) at –20°C at day 11, washed three times with PBS and blocked with 2% BSA/PBS for 30 min at room temperature. Following three washes with PBS, cells were incubated with primary antibodies for 90 min. After three washes with PBS, cells were incubated with fluorochrome-labelled secondary antibodies for 1 h under light-protected conditions. Cells were visualized by fluorescence microscopy (Axioskop, ZEISS, Jena, Germany).

Silicone substrate wrinkle assay

A thin layer of silicone fluid 200 (viscosity, 30 000 centistokes) was spread on the surface of a glass-bottom tissue culture dish (dish type; 'The optics of glass in a petri dish', MatTek, Ashland, USA). This surface was then exposed to a low flame from a Bunsen burner, allowing a film of tiny wrinkles to form on the fluid surface. The silicone took 2 s to polymerize, and was sterilized by UV exposure. Cells were added to the dishes in DMEM supplemented with 10% FCS + antibiotics and were incubated at 37°C for 1 or 2 days. Cells were then starved for 3 h with serum-free medium to exclude the well-known contractile effect of serum, followed by treatment with blebbistatin (25 μM) for 2 h. Wrinkle formation was evaluated by microscopy. Cells were then treated with endothelin-1 (ET-1; 4×10^{-8}M) for 10 min. Wrinkle formation was assessed before and after treatment with blebbistatin or ET-1.

Collagen gel contraction assay

Contraction of HSCs on collagen gel lattices was examined in six-well flat-bottom tissue culture plates (Becton Dickinson, Bedford, MA). Briefly, culture plates were pre-incubated with 2% BSA/PBS for 2 h at 37°C, washed and air-dried. Rat-tail collagen (BD Biosciences) was adjusted to physiological strength and pH with PBS and 1 M NaOH. Two millilitres of this solution (final collagen concentration: 1.5 mg·mL^{-1}) was added to each well of six-well plates. The plate was then incubated at 37°C for 1 h to allow gelatinizing. HSCs at day 13 were trypsinized, re-suspended (~0.5×10^6 cells·mL^{-1}), and plated on top of the gels (2 mL per well). After incubation overnight to allow cell attachment, serum-free conditions were introduced for 3 h. Gels were then detached from the plate by gentle circumferential dislodgment using the tip of a 200 μl pipette. Then, medium with or without blebbistatin (50 μM) was added. After 15 min, ET-1 (2×10^{-8}M) (Sigma-Aldrich) was added to elicit contraction, medium was used as a control. Twenty-four hours post treatment, gels were

photographed, the collagen gel area was measured and the 'post treatment collagen gel area' was calculated, relative to the original gel area (set to 100%).

Measurement of intracellular Ca^{2+} release
Mouse HSCs were plated on 35 mm poly-D-lysine-coated glass-bottom microwell dishes (MatTek, Ashland, MA). Measurement was carried out at day 11 on cells treated with or without blebbistatin (50 μM, 2 h) following 24 h of starvation. Cells were subsequently washed in incubation buffer, and then loaded with Fluo-4 AM (1 μM, Invitrogen) in 0.005% Pluronic F-127 (Sigma) by incubation for 25 min at 37°C. Pluronic® F-127 is a non-ionic, surfactant polyol that facilitates the solubilization of water-insoluble dyes like Fluo-4 AM. After the loading incubation, unincorporated Fluo-4 was removed by washing the coverslips. Next, ET-1 (final concentration: 4×10^{-8}M) was applied and cytosolic free Ca^{2+} was assessed by confocal laser scanning microscopy (Zeiss; LSM-510). Image data were analysed off-line using the Zeiss LSM510 analysis software V2.53.

Wound healing assay
To investigate the effect of blebbistatin on wound-induced migration, 24-well plates were coated with 5% collagen for 1.5 h at room temperature, washed three times with PBS, and blocked by 2% BSA/PBS. The 4- and 10-day-old cells were seeded at ~1×10^5 and ~5×10^4 cells per well respectively. Once the cells had attached properly, medium without FBS was added to starve the cells for 3 h. Then a 'wound' was made with a tip and medium with or without blebbistatin (0, 12.5, 25 and 50 μM) was added. Pictures were taken at the start and 24 h after 'wound induction'. Cell migration was analysed by counting the number of cells in the 'wound'.

Proliferation
Freshly isolated HSCs were replated on 96-well plate (1.6×10^4 cells per well). At day 3, medium was replaced by serum-free medium and cells were starved overnight, treated with or without blebbistatin (25 μM) for 2 h followed by stimulation with platelet-derived growth factor-BB (20 ng·mL^{-1}). After an overnight incubation, the WST-1 cell proliferation assay (Cayman, Michigan, USA) were performed according to the manufacturer's protocols.

Cell adhesion assay
24-well plates were coated with 5% collagen type I at room temperature for 2 h and blocked with 0.2% BSA/PBS at room temperature for 1 h. After trypsinization, 4- and 10-day-old cells were seeded at ~1×10^5 and ~5×10^4 cells per well respectively, and incubated for 1 h at 37°C in the presence or absence of blebbistatin (0, 12.5, 25 and 50 μM). Then, plates were washed three times with PBS to remove unattached cells. Adherent cells were stained by 0.1% crystal violet, followed by 0.2% Triton X-100 in PBS. Absorbance was measured using a microplate spectrophotometer (Bio-Rad, Hercules, USA) at a wavelength of 450 nm corrected to 595 nm.

Statistical analysis
All experiments were repeated with mouse HSCs from at least three isolations. Data were expressed as means ± a standard deviation. All statistical tests were performed using GraphPad Prism version 4.0 for Windows (GraphPad Software, San Diego, CA). One-way ANOVA (Tukey's Multiple Comparison Test) was used for collagen gel contraction and wound healing assays.

Materials
Anti-myosin IIA, anti-myosin IIB anti-α-SMA, anti-β-actin, endothelin-1 and blebbistatin were purchased from Sigma (Saint Louis, USA). 10 mM Blebbistatin stock solution was prepared in ethanol; in all experiments the control condition was medium containing vehicle control. Rat tail collagen type I was obtained from BD Biosciences (San Jose, CA, USA). Anti-rabbit IgG Alexa Fluor 488 and anti-mouse IgG Alexa Fluor 633 were purchased from Molecular Probe. Swine anti-rabbit immunoglobulins/HRP and goat anti-mouse immunoglobulins/HRP were from DAKO (Glostrup, Denmark).

Results

Effect of blebbistatin on the morphology of mouse HSCs
Culture-activated HSCs developed spreading lamellipodia and formed stress fibres. When treated with blebbistatin (0, 12.5, 25 and 50 μM) for 2 h, cells became smaller, acquired a more dendritic morphology and had less stress fibres and lamellipodia (Figure 1A). Western blot analysis showed that these changes were not due to changes in the protein expression of myosin IIA, IIB or α-SMA (Figure 1B). Myosin IIC was undetectable in mouse HSCs (data not shown). This treatment was reversible since washing the blebbistatin-treated cells with normal medium resulted in a normal HSC morphology after 24 h (Figure 1A).

Myosin IIA–α-SMA-containing stress fibres were disrupted in blebbistatin-treated HSCs
Considering that protein levels of actin and myosin II were not influenced, we studied whether the organization of myosin–actin stress fibres was altered in blebbistatin-treated cells by dual immunofluorescence staining for myosin IIA and α-SMA. Figure 2 suggests that myosin IIA and α-SMA filaments were localized in stress fibres that sometimes overlapped in control cells. When cells were treated with blebbistatin, the stress fibres disappeared. Although myosin IIA and α-SMA were still present, myosin IIA and α-SMA filaments were disrupted (Figure 2).

Silicone wrinkles do not form under blebbistatin-treated HSCs
As myosin is known to play a role in the contractility of HSCs (Saab *et al*., 2002), we investigated the effect of blebbistatin in a silicone wrinkle assay as a measure of contractility of a deformable matrix. Due to the very thin silicone film, only minimal power is needed to form wrinkles. In contrast to other techniques, such as collagen gel contraction, this assay permits the assessment of single-cell contractions. Moreover, the formation of wrinkles is reversible, allowing the analysis

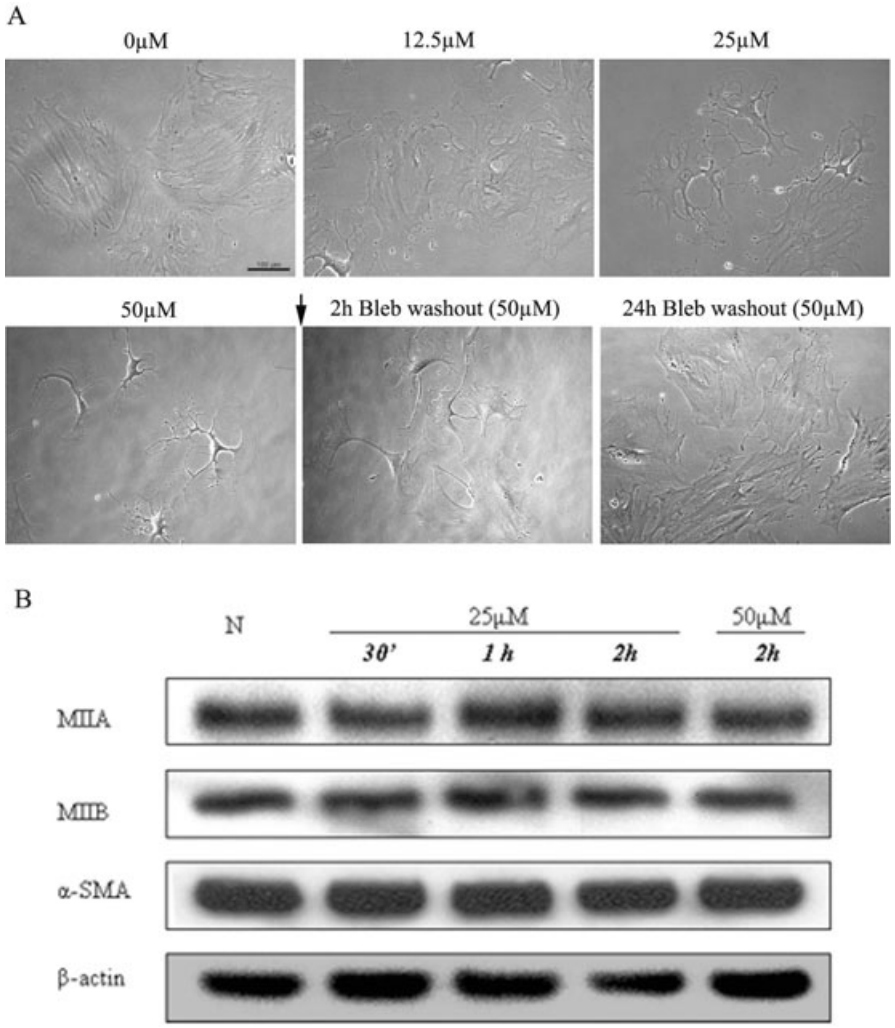

Figure 1 Effects of blebbistatin on mouse hepatic stellate cells (HSCs). (A) Phase contrast images showing that blebbistatin induced morphological changes in HSCs. Cells at day 10 were treated with or without blebbistatin (0, 12.5, 25 and 50 μM, 2 h), and removal of blebbistatin (only 50 μM shown) leads to re-appearance of normal activated HSC morphology. The scale bar represents 100 μm. (B) Western blots showing that blebbistatin did not influence protein expression. Cells at day 11 were treated with blebbistatin at different concentrations and for different periods as indicated in the figure. β-Actin was used as loading control.

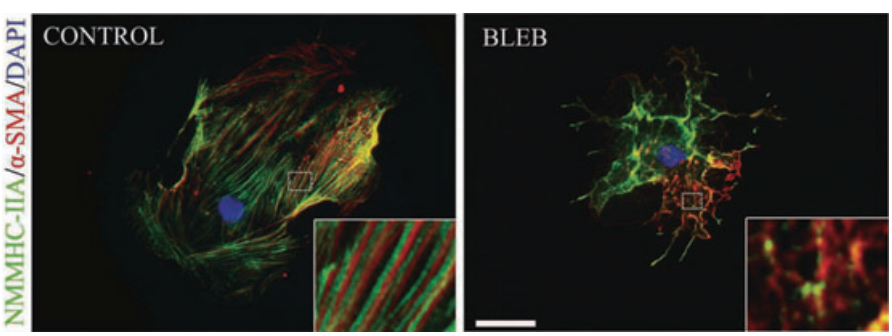

Figure 2 Blebbistatin dissociates myosin IIA – α-smooth muscle actin (α-SMA)-containing stress fibres. Cells at day 11 were treated with or without blebbistatin (50 μM) for 2 h, and then fixed in acetone/ethanol (1:3) at –20˚C for 10 min. Dual immunofluoresence staining was performed by using anti-myosin IIA (1:400) and anti-α-SMA (1:1000) antibodies. Inserts represent higher-magnification images of areas enclosed in rectangles. The scale bar represents 50 μm.

of the reversibility of drug effects. In untreated conditions, HSCs induced wrinkling of the silicone substrate, which was significantly enhanced by ET-1, a potent contractile peptide for HSCs. In contrast, cells treated with blebbistatin did not form any wrinkles in the silicone coating, not even after ET-1 stimulation (Figure 3A). Removal of blebbistatin and continued culturing of the HSCs in the presence of normal medium resulted in cells recovering and regaining their ability to form

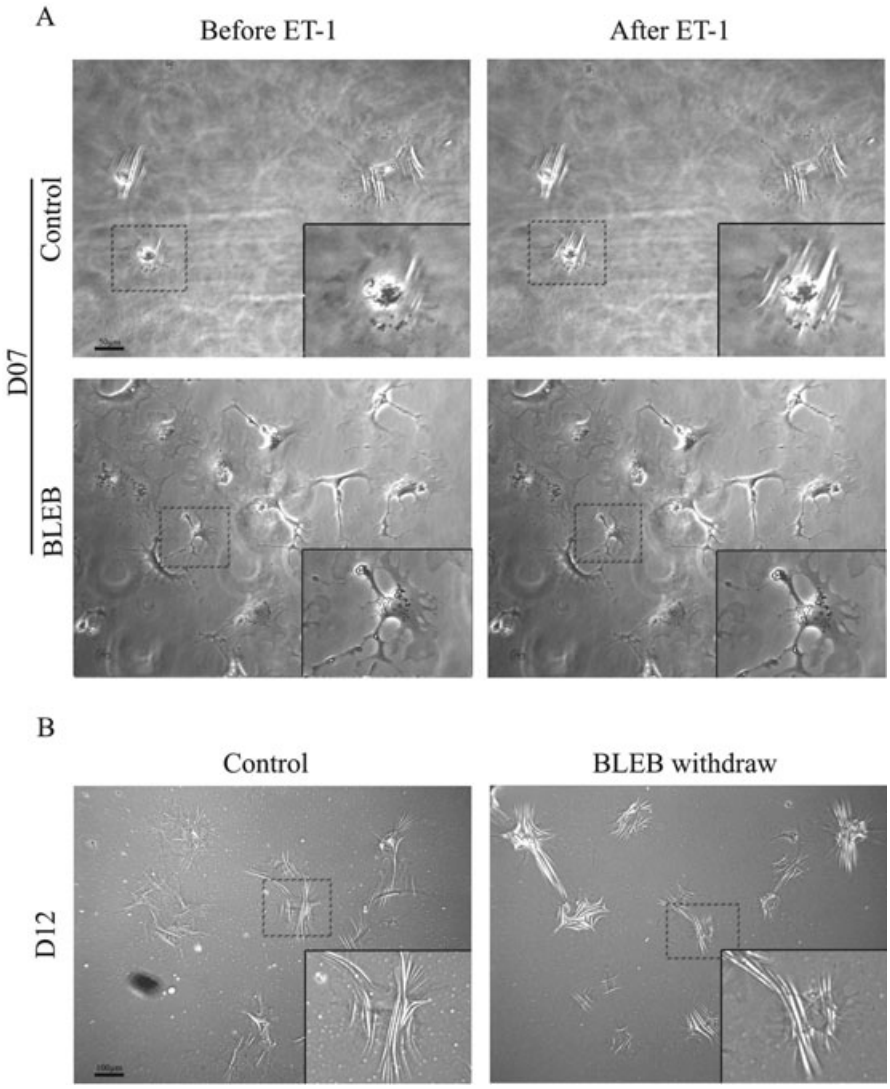

Figure 3 Blebbistatin inhibits silicone wrinkle formation, both in the presence and in the absence of the potent constrictor ET-1. (A) Mouse hepatic stellate cells (HSCs) were cultured on silicone substrate. At day 7 wrinkle formation was assessed before and after treatment with blebbistatin or ET-1. Inserts represent higher magnification images of areas marked by arrow-points in the original images. The scale bar represents 50 μm. (B) Blebbistatin was withdrawn at day 8 (no ET-1 treatment) and cell culture continued in normal medium for 4 days. Wrinkle formation was visualized at day 12. Inserts represent higher-magnification images of areas enclosed in original images. The scale bar represents 100 μm.

wrinkles. Approximately 3 days after withdrawal of blebbistatin, cells had returned to control values (Figure 3B).

Blebbistatin inhibits ET-1-induced collagen gel contraction

To further investigate the inhibitory effect of blebbistatin on HSC contraction, we performed a hydrated collagen gel assay to evaluate ET-1-induced gel contraction in the presence and absence of blebbistatin. This assay allowed us to measure the effect of blebbistatin on the contraction of a large number of HSCs. We observed in control plates that collagen fibril bundles formed around groups of cells. In the presence of blebbistatin, no or only minimal collagen fibril bundle formation was seen (Figure 4A). HSCs growing on collagen-gel resulted in a basal level of gel surface decrease of 20% (Figure 4B and C). After ET-1 stimulation, we observed a significant decrease in the gel surface (Figure 4B), the reduction being 46.5% of the original gel size (2.3 times basal level) (Figure 4C). The ET-1-induced decrease was blocked by pretreatment of the HSCs with blebbistatin (Figure 4B), resulting in a 6.9% reduction of original gel surface (Figure 4C). This shows that blebbistatin can inhibit both ET-1-induced and basal-level gel contraction by HSCs.

Intracellular Ca^{2+} release is blocked in blebbistatin-treated mouse HSCs

Because Ca^{2+} transients are involved in contraction in many cell types including activated stellate cells (Pinzani *et al.*, 1992a; Bataller *et al.*, 1998), and the cytoskeleton may be an integral component of Ca^{2+} regulation (Tseng *et al.*, 1997; Cotrina *et al.*, 1998), we measured $[Ca^{2+}]_i$ in our experimental

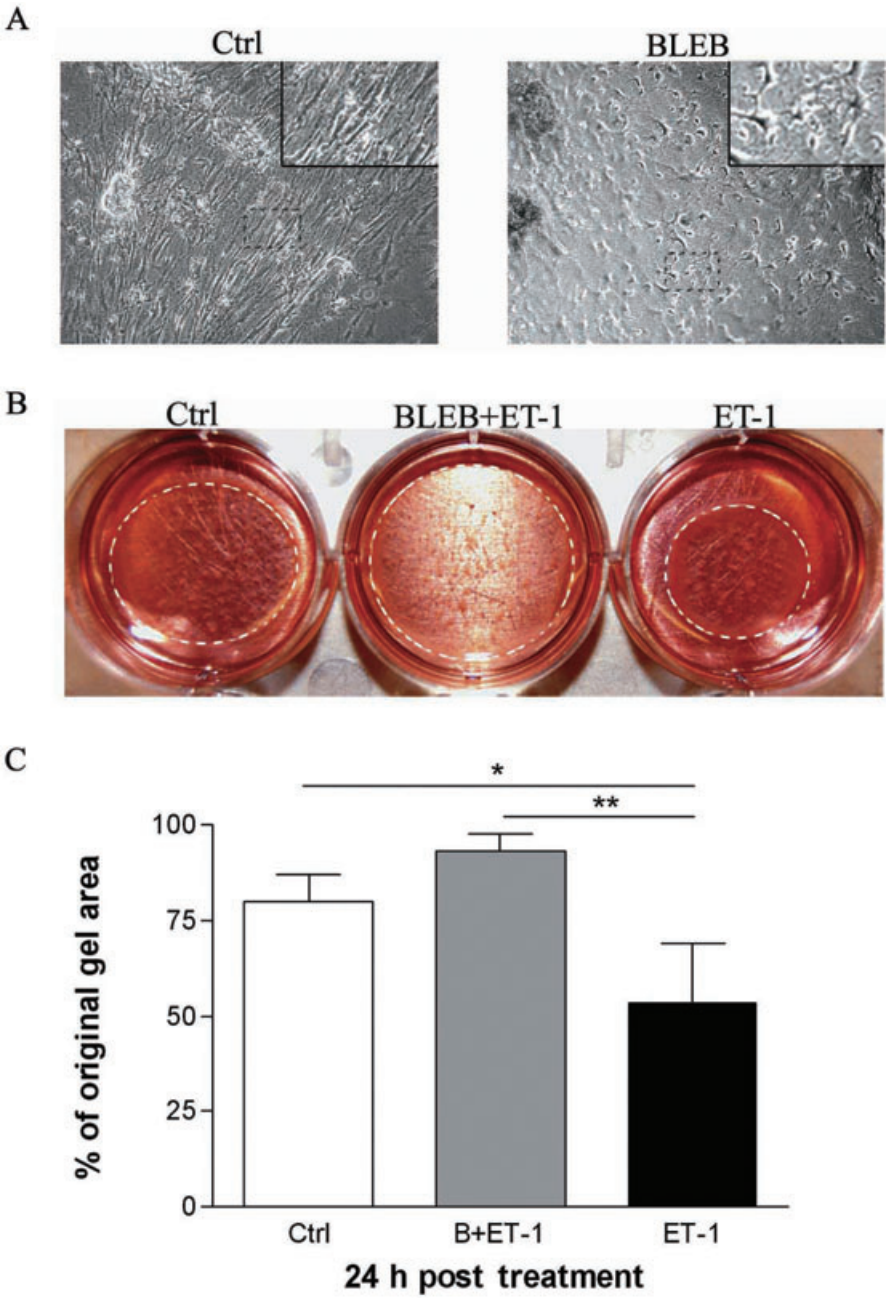

Figure 4 Blebbistatin blocks collagen gel contraction by activated hepatic stellate cells (HSCs). (A) Morphology of 14-day-cultured HSCs on collagen gel, 24 h after stimulation with 2×10^{-8} M ET-1 in the absence or presence of 50 μM blebbistatin. Inserts show collagen fibril formation (Ctrl) or the absence of collagen fibril formation (BLEB). (B) Hydrated collagen lattices, photographed 24 h after treatment. Ctrl, control medium; BLEB + ET-1, ET-1 (2×10^{-8} M) after 20 min pre-treated with blebbistatin (50 μM); ET-1, treated with ET-1 (2×10^{-8} M). Photographs represent one of three independent experiments. (C) Mean % collagen gel area compared with original collagen gel area after 24 h stimulation by ET-1 (2×10^{-8} M) with or without blebbistatin (50 μM) pre-treatment. Original gel area was normalized to 100%. Each bar represents mean and error bars represent standard deviation. Data from three independent experiments. *$P < 0.01$, relative to medium only, **$P < 0.001$, relative to ET-1.

system. HSCs were loaded with Fluo-4 and the intracellular Ca^{2+} levels were evaluated using fluorescent microscopy. Control cells showed a clear increase in $[Ca^{2+}]_i$ upon ET-1 stimulation (Figure 5A and C), while most blebbistatin-treated cells did not respond upon exposure to ET-1 (Figure 5B and C). A few cells did show a positive response to ET-1, but expressed the morphology of control cells, suggesting that these cells were not or only partially inhibited by blebbistatin (Figure 5B and C).

Blebbistatin promotes wound-induced mouse HSC migration

Following acute or chronic liver injury, HSCs are activated and migrate to sites of injury (Friedman, 2000). *In vitro*, HSCs undergo a culture-induced transdifferentiation process during which an increasing number of α-SMA containing stress fibres are formed. By cell morphological analysis and immunostaining, we rarely observed bundles of stress fibres at day 4 in culture (data not shown) while well-formed α-SMA-containing stress fibres can be easily detected in cells at day 10

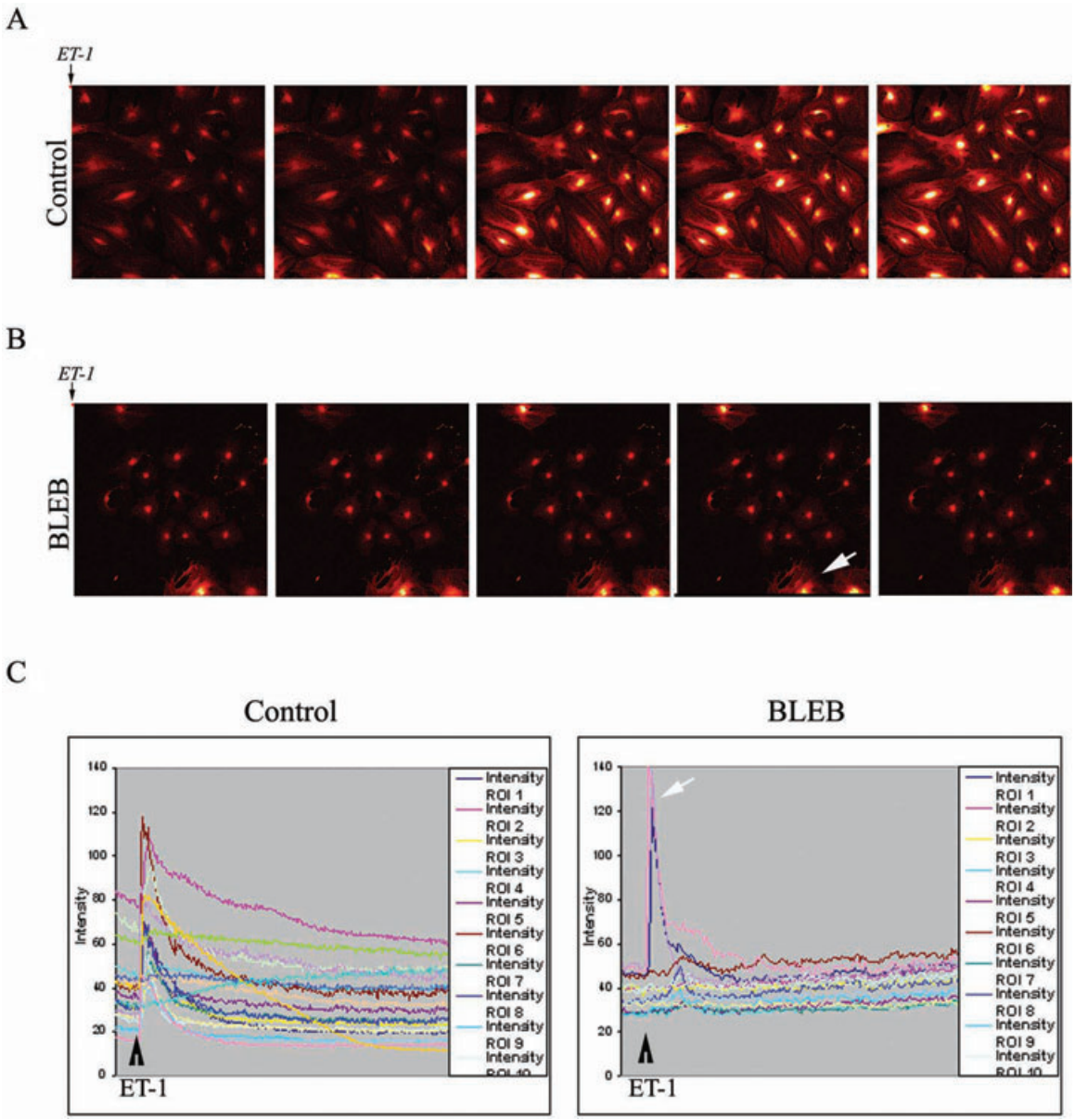

Figure 5 Blebbistatin blocks ET-1-induced intracellular Ca^{2+} release. Original fluorescence images of $[Ca^{2+}]_i$ measurements following addition of ET-1 (4×10^{-8} M) in hepatic stellate cells (HSCs) in the absence (A) or presence (B) of blebbistatin (50 μM, 2 h). Representative graph showing fluorescence intensity of $[Ca^{2+}]_i$ in response to ET-1 (C). Arrows in (B) and (C) (BLEB) point at a positively responding cell with morphology similar to that of control cells.

in culture (Figure 2). To determine the effect of blebbistatin on HSC migration, wound healing assays were performed using both day 4 and day 10 cultured HSCs. Migration of cells during wound closure was studied 24 h after scraping cells from an area in a confluent monolayer of cells. In comparison with untreated HSCs, cells treated with blebbistatin migrated faster (Figure 6A and B) and in higher numbers (Figure 6C) into the wound. This increased number was not due to proliferation in blebbistatin-treated HSC cultures (Figure 6D).

Blebbistatin decreases adhesion of activated but not quiescent HSCs to collagen type I

In view of the results of cell contraction and migration, we presumed that a reduction in stress fibres would decrease cell adhesion to collagen type I. This, in turn, would block the formation of contractile force and facilitate cell migration. Therefore, cell adhesion assays were performed with HSCs at day 4 (few stress fibres) and day 10 (fully developed stress fibres) in culture. Figure 7 clearly demonstrates that blebbistatin significantly decreased HSC adhesion at day 10 (Figure 7B), but did not influence cell adhesion at day 4 (Figure 7A).

Vinculin-containing focal adhesions disappear in blebbistatin-treated HSCs

Both classical and supermature focal adhesions have been reported in myofibroblasts and the formation and stability of supermature focal adhesions depend on high SMA-mediated

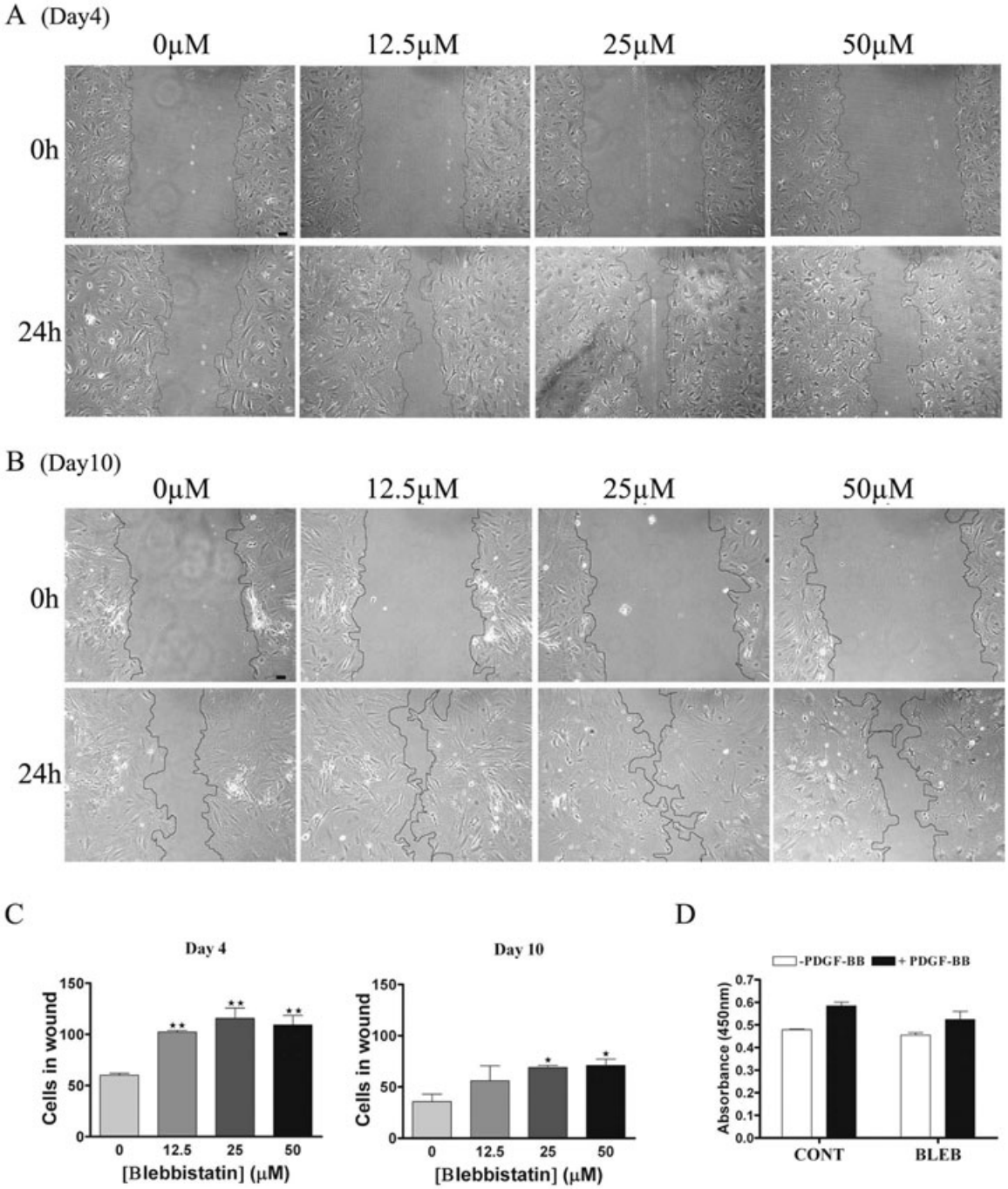

Figure 6 Wound healing assay showing that blebbistatin promotes wound-induced hepatic stellate cell (HSC) migration. (A) At day 4 after seeding, a 'wound' was made and cells were treated with blebbistatin (concentration: 0, 12.5, 25, 50 μM) at day 5. Photographs were taken at the start and 24 h after scratching. The scale bar represents 50 μm. (B) A 'wound' was made at day 10 and cells were treated with blebbistatin (0, 12.5, 25, 50 μM) at day 11. Photographs were taken at the start and 24 h after scratching. The scale bar represents 50 μm. (C) Effects of different concentrations of blebbistatin on wound-induced mouse HSC migration 24 h after treatment. Graphs show the number of cells in the wound (lower panel) and the % of area covered by migrated cells. Each bar represents means ± SD. Data from three independent experiments. $^{*}P < 0.05$, $^{**}P < 0.001$ compared with control (0 μM), the observed effect is not statistically significant for the different concentrations of blebbistatin. (D) Blebbistatin has no effect on HSC proliferation. Cell proliferation was measured by a WST-1 assay. HSCs were treated with (BLEB) or without (CONT) blebbistatin (25 μM), and in the presence or absence of platelet-derived growth factor (PDGF)-BB (20 ng·mL^{-1}).

contractile activity of myofibroblast stress fibres (Goffin *et al.*, 2006). As we showed that blebbistatin induced a disruption of stress fibres, it might be possible that it also affects focal adhesions in activated HSCs. To this end, we stained HSCs with antibodies to vinculin, which is a major component of focal adhesions. In control cells, vinculin was distributed to the cell membrane and cytoplasm to various degrees, including vinculin-containing focal adhesions organized into

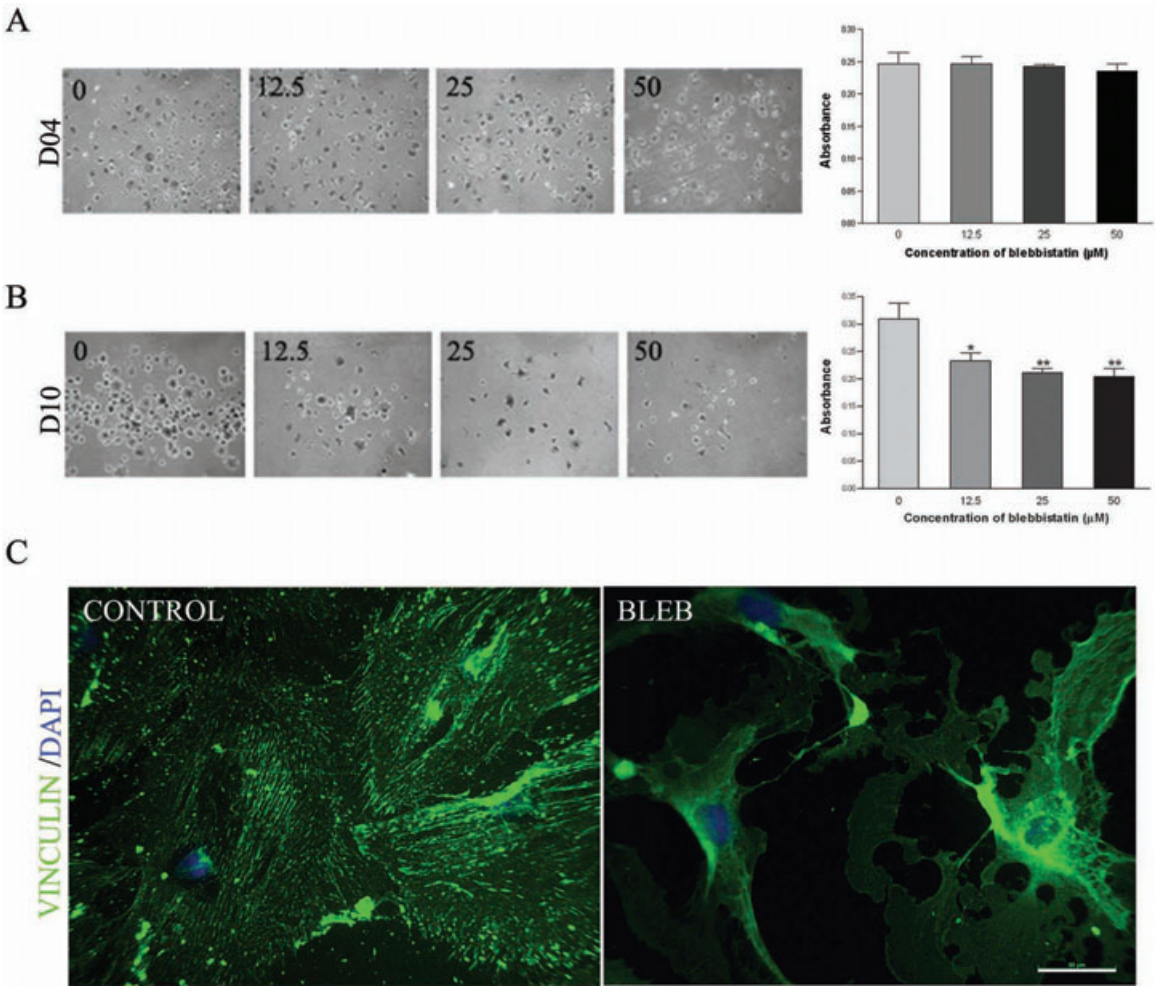

Figure 7 Cell adhesion assay. (A) Blebbistatin has no significant effect on the adhesion of quiescent hepatic stellate cells (HSCs). Images show cell adhesion after crystal violet staining of cells at day 4, treated with different concentrations of blebbistatin (0, 12.5, 25, 50 μM). Graph showing absorbance analysis of three experiments. (B) Blebbistatin decreases cell adhesion in activated HSCs. Images show cell adhesion after crystal violet staining of cells at day 10, treated with blebbistatin at different concentrations (0, 12.5, 25, 50 μM). The graph shows the absorbance analysis of three experiments. Each bar represents mean ± SD. *$P < 0.01$, **$P < 0.001$ compared with control (0 μM). The observed effect was not statistically significant for the different concentrations of blebbistatin. (C) Vinculin-containing focal adhesions disappeared in blebbistatin-treated HSCs. Cells cultured at day 11 were treated with or without blebbistatin (50 μM) for 2 h and then fixed and stained with antibodies to vinculin. The scale bar represents 50 μm.

supermature focal adhesions (Figure 7C). Treatment of the cells with blebbistatin (50 μM) for 2 h led to the disappearance of the normal distribution pattern of vinculin at the cell membrane and in most of the cytoplasm. In these blebbistatin-treated cells, vinculin showed mainly a perinuclear localization, suggesting that vinculin-containing supermature focal adhesions cannot form in the presence of blebbistatin (Figure 7C).

Discussion and conclusions

In the present study, we demonstrate that blebbistatin has profound effects on multiple aspects of the transdifferentiation of mouse HSCs, including cell morphology, focal adhesions, contraction and migration.

First, we observed a dramatic change in cell morphology after application of blebbistatin. Blebbistatin-treated mouse HSCs became smaller, had less stress fibres and acquired a dendritic morphology. Blebbistatin does not change α-SMA expression, which is a well-accepted marker protein for HSC activation (Ramadori *et al.*, 1990; Rockey *et al.*, 1992), but induces α-SMA filament disassembly, suggesting that myosin II ATPase activity is required for the regulation and stabilization of myosin-α-SMA-containing stress fibres. Those findings are consistent with studies in other cell types; for example, in rat fibroblasts, blebbistatin led to disappearance of actin–myosin bundles (Shutova *et al.*, 2008). In Caco-2 and SK-CO15 intestinal epithelial cells, inhibition of myosin II by blebbistatin resulted in decreased dynamics of cortical F-actin and induced the outgrowth of F-actin-rich surface protrusions (Ivanov *et al.*, 2008). Myosin IIA-deficient SK-CO15 cells failed to assemble F-actin stress fibres (Babbin *et al.*, 2009) and knock-down of myosin IIA expression altered epithelial cell shape and the apical F-actin appeared organized into abnormal aster-like aggregates (Ivanov *et al.*, 2007). These studies

also show a decrease in focal adhesions after a blebbistatin treatment or myosin IIA knock-down. We confirmed these observations in mouse HSC cultures in which blebbistatin decreased vinculin-containing focal adhesions in activated HSCs, which are assumed to be essential for HSCs to attach to substrates (Kawai *et al.*, 2003; Melton *et al.*, 2007). Accordingly, blebbistatin application led to reduced numbers of activated HSCs attaching to collagen substrates. This effect was amplified with increasing concentrations of blebbistatin. In contrast, blebbistatin had no such effect in quiescent HSCs, suggesting that the effect of blebbistatin on focal adhesions and mature focal cell-matrix adhesions occurs through disassembly of stress fibres. It has been reported that cells adhere to the ECM via integrin-mediated cell-matrix adhesions that link the ECM to the actin cytoskeleton. These adhesions convert the flow behind into a myosin II-driven mode. Some focal complexes can turn into elongated focal adhesions that are associated with contractile actin–myosin stress fibres (Bershadsky *et al.*, 2006). In this manner, myosin II ATPase inhibition may not suppress formation of focal complexes, but rather block their conversion into mature focal adhesions and further growth of focal adhesion. Furthermore, both classical and supermature focal adhesions occur in myofibroblasts and the formation and stability of supermature focal adhesions depend on α-SMA-containing stress fibres (Hinz *et al.*, 2003; Goffin *et al.*, 2006). These data and our results lead us to conclude that focal adhesions are different between quiescent HSCs (which have no α-SMA stress fibres) and activated HSCs (which have α-SMA stress fibres). Thus, blebbistatin decreases myosin II-α-SMA-containing stress fibres and subsequently reduces vinculin-containing mature focal adhesions. In quiescent and early activated cells without α-SMA (as day 4), cell adhesion may be related to integrin-mediated cell-matrix adhesion or other filaments, such as synemin (Uyama *et al.*, 2006).

Contraction of HSCs contributes to the regulation of sinusoidal blood flow in normal liver and to the degree of portal hypertension in cirrhosis (Rockey and Weisiger, 1996; Rockey, 2001; Marra and Pinzani, 2002; Reynaert *et al.*, 2002; Friedman, 2008). The generation of contractile force by activated HSCs in response to ET-1 has been reported in many studies (Rockey and Weisiger, 1996; Reynaert *et al.*, 2001; Saab *et al.*, 2002; Melton *et al.*, 2006). We found that ET-1-induced HSC contractility was effectively inhibited by blebbistatin both in a silicone wrinkle assay and in a collagen lattice contraction assay. Myosin II-α-SMA-containing stress fibres are major structures essential for HSC contraction (Reynaert *et al.*, 2002; Saab *et al.*, 2002). We showed that the organization of myosin–actin stress fibres was altered in blebbistatin-treated cells, which may explain the reduced contractile capability of HSCs. Two major pathways have been shown to regulate cell contraction: the Rho pathway (Yee *et al.*, 2001; Melton *et al.*, 2006) and Ca^{2+} signalling (Pinzani *et al.*, 1992b; Bataller *et al.*, 1998). In fact, Y-27632, a selective inhibitor of Rho-associated kinase and ML-7, a myosin light chain kinase inhibitor, can both inhibit myosin light chain phosphorylation, stress fibre formation and ET-1-induced contractile force generation in primary rat HSCs and a HSC cell line (Iwamoto *et al.*, 2000; Tada *et al.*, 2001; Yanase *et al.*, 2003; Melton *et al.*, 2006) and fibroblasts (Katoh *et al.*, 2001). In addition, ET-1-induced HSC contraction is elicited by an increase in intracellular Ca^{2+} (Pinzani *et al.*, 1992a; Bataller *et al.*, 1998). We did not observe an ET-1-induced $[Ca^{2+}]_i$ increase in blebbistatin-treated cells, suggesting that blebbistatin may also have an effect on HSC contraction by regulating intracellular calcium signalling. The exact mechanism is unknown, but data from different groups show that disruption of the cytoskeleton may impair $[Ca^{2+}]_i$ increase (Tseng *et al.*, 1997; Cotrina *et al.*, 1998). On the other hand, to effectively contract, cells need to attach to the ECM by means of focal adhesions (Lauffenburger and Horwitz, 1996; Melton *et al.*, 2007). We also demonstrated reduced numbers of focal adhesions in activated HSCs upon blebbistatin application.

Migration of stellate cells during hepatic injury is essential for wound healing and the development of liver fibrosis (Friedman, 2000; 2003; Melton and Yee, 2007). In HSCs, treatment with blebbistatin in both the early and later stages of activation did not inhibit – as would be expected – but rather promoted wound-induced migration. This finding is consistent with predictions of a mathematical model for cell migration (DiMilla *et al.*, 1991) and with the finding in human foreskin fibroblasts, mouse embryonic stem cells, human MCF10A breast epithelial cells and primary mouse embryonic fibroblasts, in which blebbistatin treatment or knock-down of myosin IIA also induced substantial increases in migration rates (Even-Ram *et al.*, 2007). The accelerated migration rates in mouse HSCs can be explained by several mechanisms. First, blebbistatin-induced morphological changes may facilitate cell migration (Lauffenburger and Horwitz, 1996). Second, we showed in this study that treatment with blebbistatin results in less stress fibres and mature focal adhesions, which increases cell migration by disrupting strong attachment to the underlying substrate (DiMilla *et al.*, 1991; Even-Ram *et al.*, 2007). Finally, HSCs may use a microtubule-dependent mechanism in cells lacking stress fibres and focal adhesions (Even-Ram *et al.*, 2007; Shutova *et al.*, 2008).

To our knowledge, this is the first study to report on the effects of blebbistatin on HSCs. Our results show that myosin II ATPase activity is necessary for mouse HSCs to display their characteristic contractile myofibroblast phenotype and that myosin II ATPase activity regulates important functions, such as migration and contraction, suggesting that myosin II could be a therapeutic target in the treatment of liver fibrosis and portal hypertension.

Acknowledgements

We remember Professor Albert Geerts who passed away during the finalization of this study. We are grateful to him for all his enthusiasm and support that made the realization of this project possible. This paper is in his honour. We express our warmest thanks to Jan Van Daele for assistance with confocal microscopy and Ca^{2+}-imaging, Inge Mannaerts, Eduardo Guimaraes and Sara Knops for HSC isolations, Christophe Empsen, Danielle Blijweert, Jean-Marc Lazou and Kris Derom for their technical assistance. We are grateful for support from : FWO-V (Fonds voor Wetenschappelijk Onderzoek – Vlaanderen), grants G.0512.04, G.0652.06, G.0229.08, G.0651.06; OZR (Research Council of Vrije Universiteit

Brussel) grants OZR1432BOF, OZR1149BOF, GOA48, OZR1600BOF, OZR1226, OZR1219; EASL (European Association for the Study of the Liver) 2007 Sheila Sherlock Entry Level Fellowship; I.A.P. (Belgian Science Policy Bureau) phase VI contract P6/36; IWT/SB/61314; EU 6th Framework program. Roche and Schering-Plough unconditional grant.

References

Babbin BA, Koch S, Bachar M, Conti MA, Parkos CA, Adelstein RS *et al*. (2009). Non-muscle myosin IIA differentially regulates intestinal epithelial cell restitution and matrix invasion. *Am J Pathol* **174**: 436–448.

Bataller R, Nicolas JM, Ginees P, Gorbig MN, Garcia-Ramallo E, Lario S *et al*. (1998). Contraction of human hepatic stellate cells activated in culture: a role for voltage-operated calcium channels. *J Hepatol* **29**: 398–408.

Bershadsky AD, Ballestrem C, Carramusa L, Zilberman Y, Gilquin B, Khochbin S *et al*. (2006). Assembly and mechanosensory function of focal adhesions: experiments and models. *Eur J Cell Biol* **85**: 165–173.

Calaminus SD, Auger JM, McCarty OJ, Wakelam MJ, Machesky LM, Watson SP (2007). MyosinIIa contractility is required for maintenance of platelet structure during spreading on collagen and contributes to thrombus stability. *J Thromb Haemost* **5**: 2136–2145.

Cotrina ML, Lin JH, Nedergaard M (1998). Cytoskeletal assembly and ATP release regulate astrocytic calcium signaling. *J Neurosci* **18**: 8794–8804.

DiMilla PA, Barbee K, Lauffenburger DA (1991). Mathematical model for the effects of adhesion and mechanics on cell migration speed. *Biophys J* **60**: 15–37.

Dou Y, Arlock P, Arner A (2007). Blebbistatin specifically inhibits actin-myosin interaction in mouse cardiac muscle. *Am J Physiol Cell Physiol* **293**: C1148–C1153.

Even-Ram S, Doyle AD, Conti MA, Matsumoto K, Adelstein RS, Yamada KM (2007). Myosin IIA regulates cell motility and actomyosin-microtubule crosstalk. *Nat Cell Biol* **9**: 299–309.

Farman GP, Tachampa K, Mateja R, Cazorla O, Lacampagne A, de Tombe PP (2008). Blebbistatin: use as inhibitor of muscle contraction. *Pflugers Arch* **455**: 995–1005.

Fedorov VV, Lozinsky IT, Sosunov EA, Anyukhovsky EP, Rosen MR, Balke CW *et al*. (2007). Application of blebbistatin as an excitation-contraction uncoupler for electrophysiologic study of rat and rabbit hearts. *Heart Rhythm* **4**: 619–626.

Friedman SL (2000). Molecular regulation of hepatic fibrosis, an integrated cellular response to tissue injury. *J Biol Chem* **275**: 2247–2250.

Friedman SL (2003). Liver fibrosis – from bench to bedside. *J Hepatol* **38** (Suppl 1): S38–S53.

Friedman SL (2008). Hepatic stellate cells: protean, multifunctional, and enigmatic cells of the liver. *Physiol Rev* **88**: 125–172.

Geerts A (2001). History, heterogeneity developmental biology and functions of quiescent hepatic stellate cells. *Semin Liver Dis* **21**: 311–335.

Goffin JM, Pittet P, Csucs G, Lussi JW, Meister JJ, Hinz B (2006). Focal adhesion size controls tension-dependent recruitment of alpha-smooth muscle actin to stress fibers. *J Cell Biol* **172**: 259–268.

Gressner AM (1991). Liver fibrosis: perspectives in pathobiochemical research and clinical outlook. *Eur J Clin Chem Clin Biochem* **29**: 293–311.

Guha M, Zhou M, Wang YL (2005). Cortical actin turnover during cytokinesis requires myosin II. *Curr Biol* **15**: 732–736.

Haviv L, Gillo D, Backouche F, Bernheim-Groswasser A (2008). A cytoskeletal demolition worker: myosin II acts as an actin depolymerization agent. *J Mol Biol* **375**: 325–330.

Hinz B, Dugina V, Ballestrem C, Wehrle-Haller B, Chaponnier C (2003). Alpha-smooth muscle actin is crucial for focal adhesion maturation in myofibroblasts. *Mol Biol Cell* **14**: 2508–2519.

Ivanov AI, Bachar M, Babbin BA, Adelstein RS, Nusrat A, Parkos CA (2007). A unique role for nonmuscle myosin heavy chain IIA in regulation of epithelial apical junctions. *PLoS One* **2**: e658.

Ivanov AI, Hopkins AM, Brown GT, Gerner-Smidt K, Babbin BA, Parkos CA *et al*. (2008). Myosin II regulates the shape of three-dimensional intestinal epithelial cysts. *J Cell Sci* **121**: 1803–1814.

Iwamoto H, Nakamuta M, Tada S, Sugimoto R, Enjoji M, Nawata H (2000). A p160ROCK-specific inhibitor, Y-27632, attenuates rat hepatic stellate cell growth. *J Hepatol* **32**: 762–770.

Katayama T, Yoshiyama S, Tanaka H, Wang HH, Nakamura A, Kohama K (2006). Blebbistatin inhibits sphingosylphosphorylcholine-induced contraction of collagen-gel fiber populated by vascular smooth-muscle cells. *J Pharmacol Sci* **102**: 339–342.

Katoh K, Kano Y, Amano M, Kaibuchi K, Fujiwara K (2001). Stress fiber organization regulated by MLCK and Rho-kinase in cultured human fibroblasts. *Am J Physiol Cell Physiol* **280**: C1669–C1679.

Kawai S, Enzan H, Hayashi Y, Jin YL, Guo LM, Miyazaki E *et al*. (2003). Vinculin: a novel marker for quiescent and activated hepatic stellate cells in human and rat livers. *Virchows Arch* **443**: 78–86.

Lauffenburger DA, Horwitz AF (1996). Cell migration: a physically integrated molecular process. *Cell* **84**: 359–369.

Limouze J, Straight AF, Mitchison T, Sellers JR (2004). Specificity of blebbistatin, an inhibitor of myosin II. *J Muscle Res Cell Motil* **25**: 337–341.

Marra F, Pinzani M (2002). Role of hepatic stellate cells in the pathogenesis of portal hypertension. *Nefrologia* **22** (Suppl 5): 34–40.

Melton AC, Yee HF (2007). Hepatic stellate cell protrusions couple platelet-derived growth factor-BB to chemotaxis. *Hepatology* **45**: 1446–1453.

Melton AC, Datta A, Yee, HF, Jr. (2006). [Ca2+]i-independent contractile force generation by rat hepatic stellate cells in response to endothelin-1. *Am J Physiol Gastrointest Liver Physiol* **290**: G7–G13.

Melton AC, Soon RK, Jr., Park, JG, Martinez L, Dehart GW, Yee, HF, Jr. (2007). Focal adhesion disassembly is an essential early event in hepatic stellate cell chemotaxis. *Am J Physiol Gastrointest Liver Physiol* **293**: G1272–G1280.

Pinzani M, Failli P, Ruocco C, Casini A, Milani S, Baldi E *et al*. (1992a). Fat-storing cells as liver-specific pericytes. Spatial dynamics of agonist-stimulated intracellular calcium transients. *J Clin Invest* **90**: 642–646.

Pinzani M, Failli P, Ruocco C, Casini A, Milani S, Baldi E *et al*. (1992b). Fat-storing cells as liver-specific pericytes. Spatial dynamics of agonist-stimulated intracellular calcium transients. *J Clin Invest* **90**: 642–646.

Ramadori G, Veit T, Schwogler S, Dienes HP, Knittel T, Rieder H *et al*. (1990). Expression of the gene of the alpha-smooth muscle-actin isoform in rat liver and in rat fat-storing (ITO) cells. *Virchows Arch B Cell Pathol Incl Mol Pathol* **59**: 349–357.

Reynaert H, Thompson MG, Thomas T, Geerts A (2002). Hepatic stellate cells: role in microcirculation and pathophysiology of portal hypertension. *Gut* **50**: 571–581.

Reynaert H, Vaeyens F, Qin H, Hellemans K, Chatterjee N, Winand D *et al*. (2001). Somatostatin suppresses endothelin-1-induced rat hepatic stellate cell contraction via somatostatin receptor subtype 1. *Gastroenterology* **121**: 915–930.

Rockey DC (2001). Hepatic blood flow regulation by stellate cells in normal and injured liver. *Semin Liver Dis* **21**: 337–349.

Rockey DC, Weisiger RA (1996). Endothelin induced contractility of stellate cells from normal and cirrhotic rat liver: implications for regulation of portal pressure and resistance. *Hepatology* **24**: 233–240.

Rockey DC, Boyles JK, Gabbiani G, Friedman SL (1992). Rat hepatic lipocytes express smooth muscle actin upon activation in vivo and in culture. *J Submicrosc Cytol Pathol* **24**: 193–203.

Rosner H, Moller W, Wassermann T, Mihatsch J, Blum M (2007).

Attenuation of actinomyosinII contractile activity in growth cones accelerates filopodia-guided and microtubule-based neurite elongation. *Brain Res* **1176**: 1–10.

Saab S, Tam SP, Tran BN, Melton AC, Tangkijvanich P, Wong H *et al*. (2002). Myosin mediates contractile force generation by hepatic stellate cells in response to endothelin-1. *J Biomed Sci* **9**: 607–612.

Salhia B, Hwang JH, Smith CA, Nakada M, Rutka F, Symons M *et al*. (2008). Role of myosin II activity and the regulation of myosin light chain phosphorylation in astrocytomas. *Cell Motil Cytoskeleton* **65**: 12–24.

Sellers JR (2000). Myosins: a diverse superfamily. *Biochim Biophys Acta* **1496**: 3–22.

Shu S, Liu X, Korn ED (2005). Blebbistatin and blebbistatin-inactivated myosin II inhibit myosin II-independent processes in. Dictyostelium. *Proc Natl Acad Sci USA* **102**: 1472–1477.

Shutova MS, Alexandrova AY, Vasiliev JM (2008). Regulation of polarity in cells devoid of actin bundle system after treatment with inhibitors of myosin II activity. *Cell Motil Cytoskeleton* **65**: 734–746.

Straight AF, Cheung A, Limouze J, Chen I, Westwood NJ, Sellers JR *et al*. (2003). Dissecting temporal and spatial control of cytokinesis with a myosin II Inhibitor. *Science* **299**: 1743–1747.

Tada S, Iwamoto H, Nakamuta M, Sugimoto R, Enjoji M, Nakashima Y *et al*. (2001). A selective ROCK inhibitor, Y27632, prevents dimethylnitrosamine-induced hepatic fibrosis in rats. *J Hepatol* **34**: 529–536.

Tseng S, Kim R, Kim T, Morgan KG, Hai CM (1997). F-actin disruption attenuates agonist-induced [Ca2+], myosin phosphorylation, and force in smooth muscle. *Am J Physiol* **272**: C1960–C1967.

Uyama N, Zhao L, Van RE, Hirako Y, Reynaert H, Adams DH *et al*. (2006). Hepatic stellate cells express synemin, a protein bridging intermediate filaments to focal adhesions. *Gut* **55**: 1276–1289.

Wang HH, Tanaka H, Qin X, Zhao T, Ye LH, Okagaki T *et al*. (2008). Blebbistatin inhibits the chemotaxis of vascular smooth muscle cells by disrupting the myosin II-actin interaction. *Am J Physiol Heart Circ Physiol* **294**: H2060–H2068.

Yanase M, Ikeda H, Ogata I, Matsui A, Noiri E, Tomiya T *et al*. (2003). Functional diversity between Rho-kinase- and MLCK-mediated cytoskeletal actions in a myofibroblast-like hepatic stellate cell line. *Biochem Biophys Res Commun* **305**: 223–228.

Yee HF, Jr., Melton, AC, Tran BN (2001). RhoA/rho-associated kinase mediates fibroblast contractile force generation. *Biochem Biophys Res Commun* **280**: 1340–1345.

Zhang M, Rao PV (2005). Blebbistatin, a novel inhibitor of myosin II ATPase activity, increases aqueous humor outflow facility in perfused enucleated porcine eyes. *Invest Ophthalmol Vis Sci* **46**: 4130–4138.